

## Applications of an analytical method to calculate the load distribution along a fibre in a loaded network

WARREN BATCHELOR

Australian Pulp and Paper Institute, Department of Chemical Engineering, Monash University

### ABSTRACT

A new analytical solution for the load distribution along a fibre in a network has been used to investigate some aspects of paper tensile strength and elastic modulus. The method uses a similar approximation to the shear-lag formulation but allows stress transfer at individual contacts, rather than specifying a single stress transfer function applying along the entire length of the fibre. Measured elastic modulus data, where the fibres only varied in length and not cross-section showed only a small effect of fibre length on modulus. This is consistent with a high overall stress transfer coefficient for each fibre-fibre contact, resulting in the contacts at the ends of the fibres being heavily loaded. The maximum force at the middle of the fibre was calculated as a function of the fibre-fibre shear bond strength. The data showed that most literature values are too low to allow the fibre to break during paper fracture. The simulation method was able to explain the reduction in sheet tensile strength with a reduction in density, but was unable to explain the reduction in sheet strength with reduced fibre length. The assumption that a fibre-fibre bond fails completely once its breaking load is exceeded is believed to cause the discrepancy.

### INTRODUCTION

Paper mechanical properties include strength, elastic modulus and stretch at break. Strength and stiffness are very important for paper performance in many converting and end-use applications.

Paper itself is a network of ligno-cellulosic fibres bonded together through hydrogen bonds. The fibres are positioned stochastically, that is with their centres randomly located, and with orientation determined according to an orientation distribution. Additional perturbing influences on fibre location are flocculation, where fibre clumping produces local areas of high grammage, with corresponding areas of low grammage elsewhere in the sheet. Acting in opposition to this tendency, fibres may also be more uniform than would be predicted from randomly located positions, since areas of low grammage will experience greater drainage during sheet formation, concentrating fibres at that point, a process known as self-healing. The orientation and distribution of fibres in contact with any given fibre

of interest are determined by the overall stochastic distribution as well as influences from flocculation and self-healing. For a stochastic three dimensional network, distances between contacting fibres have been shown to be given by a  $\Gamma$  function (1), while experimental data (2) have been fitted by a two-parameter Weibull probability density function yielding similarly shaped distributions

$$f(x_n - x_{n-1}) = \left( (x_n - x_{n-1}) / b \right)^{c-1} \cdot \left( \exp(-(x_n - x_{n-1}) / b) \right)^{c/b} \quad (1)$$

where  $b$  and  $c$  are constants, and  $b, c > 0$ , and  $x_n - x_{n-1} \geq 0$ . Increasing paper non-uniformity, through increasing flocculation, reduces paper strength through fracture in low grammage areas (3, 4). The effect of the non-uniformity of the structure at the fibre level on paper mechanical properties has never been investigated in detail.

When a fibre network, such as paper, is elastically loaded, the total force developed at a given elastic strain can be summed from the components of the forces in the individual fibres in the stress direction. These are controlled by the fibre elastic modulus and dimension, the fibre-fibre contacts and the stress transfer from the fibrous network through the contacting fibres into each individual fibre. Our current understanding of stress-transfer within fibrous networks is incomplete and only limited measurements of fibre elastic modulus have been completed.

As well as the factors controlling the elastic modulus, paper strength is also controlled by fibre strength and the fibre-fibre shear bond strength. Fibres surfaces are bonded together with hydrogen bonds. No theoretical prediction of bond strength is available. Experimental measurements have been conducted using a wide variety of techniques to prepare the bonds. Values have also been estimated by using the bond strength as a fitting parameter in the Page equation for paper strength (5, 6). A review (7) of the available values found that measured and theoretically derived shear bond strengths ranged from 2 to 25 MPa. It appears to be extremely difficult to prepare bonds representative of those found in a sheet as well as to prevent out of plane deformation and twisting while testing the bonds. Some measurements of single fibre strength have been conducted, although the measurements are extremely tedious and so zero-span strength is preferred. Zero-span strength is imperfect in that it is measured on the sheet and is an average only as well as being affected by sheet grammage (8). The zero-span strength will fall with increasing grammage due to the stress transfer mechanism into the sample (9). Assuming that the density of the fibre wall is  $1500 \text{ kg/m}^3$ , it

can be shown using Van den Akker's result for an isotropic sheet (10) that fibre strength,  $\sigma_f$ , is related to zero-span strength,  $Z$ , by  $\sigma_f = 4Z$ , when  $\sigma_f$  is expressed in MPa and zero-span strength is expressed as kNm/kg.

One interesting aspect of the elastic modulus and strength of paper that has received relatively little attention is the dependence of these properties on fibre length. According to data from Japanese researchers given in page 145 in Niskanen (11), elastic modulus depends only slightly on fibre length, provided all other cross-sectional dimensions are held constant, whereas paper strength depends strongly on fibre length. This should be further investigated since theories of both elastic modulus and strength include fibre length.

The first theory for the elastic modulus of paper is due to Cox (12), who treated paper as a fibre reinforced composite. Cox showed that for a randomly oriented sheet of fibres with length,  $l$ , the elastic modulus of the sheet is a third of the component fibres. If the fibres are finite in length then, assuming that the stress transferred into a fibre over an interval  $[x, dx]$  from the matrix is proportional to the displacement of position  $x$  relative to the overall strain the matrix, it was shown that the effective fibre modulus was reduced by  $1 - \tanh(\beta l/2)/(\beta l/2)$ , where  $l$  was the fibre length and  $\beta$  was a constant related to the stress transfer efficiency into the fibre and the fibre elastic modulus and cross-sectional area. The reduction in effective elastic modulus is due to the ends of the fibre being less heavily loaded than the middle of the fibre. The shear-lag model has been further extended to qualitatively include defects in fibres (13, 14) and found to accurately match the form of average stress distributions along fibres obtained from a finite element model of a thin network (15). None of these models consider paper made from fibres with distributions of dimensions and mechanical properties. Räisänen et al have further criticised the shear-lag model on the grounds that the direct stress transfer from fibres with low crossing angles is likely to be the dominant mode of transfer, rather than by shear of perpendicularly oriented fibres (16).

Analytical models for paper strength include the Page equation (17), the Shallhorn Karnis model (18) based on theory of the failure of composites and one based on shear-lag theory by Carlsson and Lindström (19). All models assume uniform, straight fibres. Interestingly the stress transfer mechanism on all three models is quite different to the stress transfer for the shear-lag model of elastic modulus. The shear-lag model for elastic modulus

has the highest stress transfer into the fibre at ends, reducing towards the middle as the strain in the fibre approaches the network strain asymptotically. However the models for strength all assume a uniform increase to a sharp peak from the ends of the fibre to the mid-point. This is justified explicitly in the work by Carlsson and Lindström as arising from complete yielding of the matrix along the length of the fibre, as proposed originally by Kelly and Tyson (20). In the work of Page, this is stated without justification.

There is still discussion as to what actually triggers the failure of paper. When paper fails, a fibre crossing the fracture line can either break or pull-out. Microscopic examination of fractures lines shows that both pull-out and fracture occur in paper under normal conditions (21) and that bonds start to fail prior to the actual failure of the sample. Page assumed that fibres that pull out have failed completely before final failure and thus carry no load at the point of fracture, hence it is the failure of the fibres which triggers final fracture. Carlsson and Lindström appear to have assumed that both fibre failure and pull-out occur simultaneously. The issue is important as whether the fibres fracture or pull-out will control the subsequent evolution of the fracture zone and the stability of the fracture process.

The preceding discussion has demonstrated that there are still a large number of outstanding issues in paper mechanics. While progress has been made with theory, allowing us to qualitatively understand the influence of fibre and network properties on strength and modulus, it has not been possible to incorporate variability in fibre and structure or even to prove that it is not necessary to consider such variability. It is the purpose of this paper to apply a recently published method (22) to examine some of the outstanding issues in paper mechanics. The method considers paper as being composed of three components- a single fibre of interest, which is connected to a uniform matrix by a set of crossing fibres. The model uses the shear-lag assumption of linear coupling between the force generated at a contact and the displacement of the contact relative to the uniform matrix. However the model differs from the shear-lag in that the equations are solved for discrete contacts, each with independent stress transfer coefficient, rather than a single uniform stress transfer coefficient. In this paper, I will use this model to examine what fibre-fibre bond strength is compatible with some fibres breaking upon sheet fracture, as is observed experimentally. I will also examine the effect of the variability in the number of contacts and positions caused by the stochastic fibre structure as well as investigating the reasons why elastic modulus has been reported

to be largely insensitive to fibre length, while tensile strength depends strongly on fibre length.

### THEORY

What follows is a summary of the derivation given in (22), which should be consulted for further information. The analysis starts with half a fibre, which is connected to an external fibre network by  $i$  contact points. The fibre is assumed to be linear elastic. The centre of the fibre at  $x_0 = 0$  is set as the reference point and it is assumed that the force distribution is symmetric around the mid-point. A strain of  $\varepsilon$  in the direction of the fibre axis is applied to the external network and force is transferred into the fibre by displacements of the contact points from their equilibrium position for the applied network strain. The displacement of the  $j^{\text{th}}$  contact is designated  $\delta_j$ . The forces that develop at the  $j^{\text{th}}$  contact are assumed to linearly related to  $\delta_j$  by a stress transfer coefficient,  $\beta_j$ , such that

$$F_j = \beta_j \delta_j \quad (2)$$

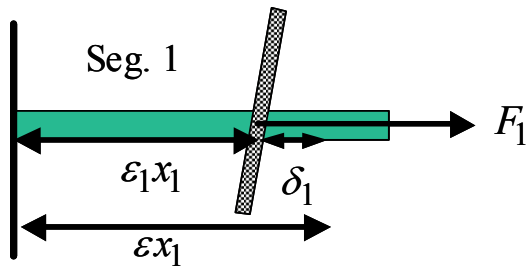


Figure 1. Displacement of the first crossing point at position,  $x_1$ , from equilibrium position in the applied strain field,  $\varepsilon$ .

The idea is illustrated in Figure 1, which shows segment 1 of the loaded fibre, running from the midpoint of the fibre at  $x_0 = 0$  to the position of the first contact,  $x_1$ . This has a strain in the first segment of  $\varepsilon_1$  which differs from the network strain,  $\varepsilon$ , displacing the crossing point from the equilibrium position by  $\delta_1 = (\varepsilon_1 - \varepsilon)(x_1 - x_0)$ . The force which has produced the strain  $\varepsilon_1$  is the sum of the forces developed at all  $i$  crossing fibres and therefore

$$\delta_1 = \frac{(x_1 - 0)}{E_1 A_1} \sum_{j=1}^{j=i} \beta_j \delta_j - \varepsilon (x_1 - 0) \quad (3)$$

where  $E_1$  and  $A_1$  are the elastic modulus and cross-sectional area, respectively, of segment 1. Each segment is assumed to have a constant cross-section and elastic modulus, but these can be set independently for each segment.

The displacement at the second contact is the sum of the displacement in the first and second segments which gives

$$\delta_2 = (x_1 - 0) \left( \frac{\sum_{j=1}^{j=i} \beta_j \delta_j}{E_1 A_1} - \varepsilon \right) + (x_2 - x_1) \left( \frac{\sum_{j=2}^{j=i} \beta_j \delta_j}{E_2 A_2} - \varepsilon \right) \quad (4)$$

which may be rewritten as

$$\delta_1 = \delta_2 - (x_2 - x_1) \left( \frac{\sum_{j=2}^{j=i} \beta_j \delta_j}{E_2 A_2} - \varepsilon \right) \quad (5)$$

Extending this reasoning it can be shown that for the  $n-1^{\text{th}}$  and  $n^{\text{th}}$  contacts that

$$\delta_{n-1} = \delta_n - (x_n - x_{n-1}) \left( \frac{\sum_{j=n}^{j=i} \beta_n \delta_n}{E_n A_n} - \varepsilon \right) \quad (6)$$

Thus  $\delta_{i-1}$ , can be written in terms of  $\delta_i$ ;  $\delta_{i-2}$  can be written in terms of  $\delta_{i-1}$  and thus in terms of  $\delta_i$ , and a similar chain can be developed such that each displacement can be expressed in terms of  $\delta_i$ , the displacement at the final crossing nearest the fibre end. The displacements at all the fibre crossings can be expressed in terms of  $\delta_i$  and as  $\delta_i$  is given by

$$\delta_i = \sum_{k=1}^{k=i} \frac{(x_k - x_{k-1})}{E_k A_k} \left( \sum_{j=k}^{j=i} \beta_j \delta_j \right) - \varepsilon x_i \quad (7)$$

then it is possible to solve this equation to determine  $\delta_i$  and thus to uniquely determine the displacements at all crossings. This solution will be exact under the specified assumptions.

The advantages of this approach over the shear-lag approach, which is the starting point for the derivation of these equations, are that each contact position, and stress transfer coefficient can be independently specified. The cross-sectional area and elastic modulus of each segment can also be independently specified. Thus the effect of the stochastic paper structure can be modelled by generating distances between contacts according to measured distributions. Non-uniformities along a fibre, such as changes in cross-sectional dimensions or defects can also be modelled. The main disadvantage of the method is that it limited to linearly elastic fibres, while paper is elastic-plastic and can show considerable plastic deformation at failure.

In the work presented here I have not attempted to model the strength of paper. There are still a

number of issues that need to be resolved, before this can be completed. In particular, real paper structures will have contacts that are a mixture of full contacts and partial contacts (2). The partial contacts are produced when fibres become twisted during pulping and sheet manufacture. One of the effects of wet-pressing is to untwist and flatten fibres (23). These effects still need to be considered for incorporation into the model. Rather, the work here will demonstrate the utility of the method and provide insight into some of the major open questions in paper mechanics.

## EXPERIMENTAL DATA

The experimental data were all collected as part of a PhD thesis investigating the factors affecting paper strength (24). The starting material was an unbleached, never dried, laboratory cooked radiata pine kraft with a kappa number of 30, which is labelled L0. This type of pulp is an important research tool because it produces fibres that are as straight and free from defects as possible. The fibre length was altered by forming sheets from the starting stock, cutting them while still wet and then reslushing the sheets, before making fibres. Three levels of cutting were used to create sheets denoted L1-L3. The wet-cutting operation reduced the length of the fibres while preserving the cross-sectional area and dimensions. For each sample, isotropic 60 gsm sheets were made on a laboratory sheet former and pressed at five different pressing levels, in order to vary the level of bonding in the sheet, however only the sheets made at the middle pressing level (P3) are presented here. Zero-span strength was measured on a Pulmac Troubleshooter. Further details are available in (24).

The fibre cross-sectional area and width was measured in the sheet using a combination of resin embedding and confocal microscopy (25). Fibre width was estimated from the width of the smallest rectangular bounding box that could be fitted around the irregular shape of the fibre (25). The dimensions of the bounding box are  $D_h$  and  $D_w$ . The summary data for the fibre dimensions for the samples used in the simulations presented here are shown in Table 1.

Table 1 Fibre dimensions and sheet density for samples used in simulations

Sample	X-sect. Area ( $\mu\text{m}^2$ )	$D_w$ ( $\mu\text{m}$ )	$D_h$ ( $\mu\text{m}$ )	Density ( $\text{kg}/\text{m}^3$ )	Fibre length (mm)
L0 P3	198	30.7	12.3	509	3.14
L1 P3	207	34.5	12.1	522	2.53
L2 P3	199	33.1	11.5	434	2.10
L3 P3	N.A.	N.A.	N.A.	470	1.79

Table 2 Weibull distribution parameters for fibre-fibre contact distances, fraction of full contacts and fibre breaking force calculated from the zero (Z) span tensile index, for samples used in the simulations.

Sample name	Weibull b	Weibull c	Frac full contacts	Z-span index (Nm/g)	Fibre break force (N)
L0 P3	48.4	1.62	0.48	148.6	0.129
L1 P3	53.4	1.58	0.53	151.9	0.138
L2 P3	53.7	1.50	0.49	148.2	0.130
L3 P3	N.A.	N.A.	N.A.	155.8	0.136

The fibre-fibre contacts on some samples were also measured by examining fibres sectioned longitudinally by the sheet cross-section (2) and directly counting fibres in contact. Fibres in contact were either assigned as full or partial contacts, depending on whether contact was made across the full width of the contacting fibre or not. Partial contacts arise because the fibres become twisted during the sheet making process. The distances between fibre contact centres were measured and fitted by a two-parameter Weibull probability density function (PDF), as given by equation 1. The fibre contact data as well as the zero-span tensile index data are given in Table 2. Table 2 also gives the fibre breaking force estimated from the zero-span tensile strength, increased by 10% to account for non-linear stress transfer under the jaws (8).

Since only the data from the third level of pressing (P3) was used, the shortcuts L0, L1 etc only are used, without the pressing level. The fibre elastic modulus is a parameter required for simulations. This was assumed to be 30 GPa, based on literature data (26), as no data was available for the samples tested.

## RESULTS

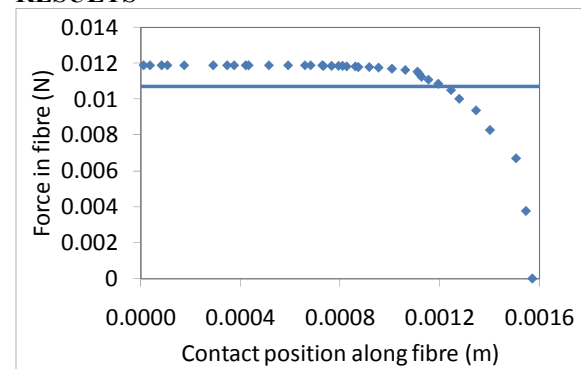


Figure 2 Single calculated force curve along a fibre from sample L0 with sheet density 509  $\text{kg}/\text{m}^3$ .

Figure 2 shows a single force distribution curve along half a fibre for sample L0. This figure has

been included to show the types of curves that the simulation generates. The set of contacts has been randomly generated from the contact statistics given in Table 1. A stress transfer coefficient  $\beta$  of 15,000 and an external network strain of 0.2% were used. The reasons for the selection of this stress transfer coefficient are discussed later. Each point on this curve is a single contact point and the force at the contact point gives the load in the fibre segment to the left of the contact. For a pair of adjacent points, subtracting the force on the RHS from that on the LHS gives the force applied at the RHS contact. The general shape of the curve in Figure 2, with build up of stress at the ends of the fibre, approaching an asymptotic stress value at the middle is very similar to that predicted by shear-lag theory. This is not surprising given that the same underlying mechanism of stress transfer applies in both cases. The difference between the two is that the shear lag equations give a smooth asymptotic approach to a limit, while the solution with discrete contacts does not. The important data generated from this solution are the average force of 0.0107N, which is indicated by the solid line on the graph, the maximum force at the middle of the fibre of 0.0119 and the force at each contact. The maximum force at a contact is at the last contact at the end of the fibre, which had a load of 0.0038N. Providing the fibre orientation distribution and sheet grammage are held constant, the force in the network will be proportional to the average force along the fibre.

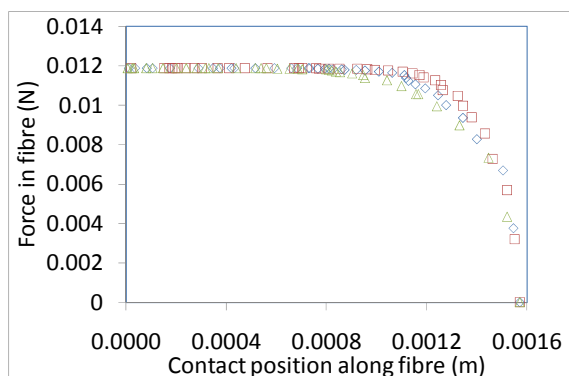


Figure 3 Three simulations for sample L0 with sheet density of 509 kg/m<sup>3</sup>

Figure 3 shows three separate simulations for L0. The simulations produced 36, 37 and 38 contacts for each fibre. The number of contacts is reasonably uniform because the sheet is reasonably dense, with a density of 509 kg/m<sup>3</sup>, and the Weibull distribution of fibre-fibre contact distances is compressed compared to a lower sheet density. The data all have the same final maximum force at the middle of the fibre. However the development of force at the end of the fibre is different between the simulations. This entirely reflects the density of fibre-fibre contacts, and their positions, at the

end of the fibre. It can be seen also that the force at the final contact at the end of the fibre is different between the simulations. There were small differences between the average forces for the whole fibre for the three simulations. That data shows that the local environment is important to the calculated force distribution. It is not sufficient to only employ average contact distances, such as are incorporated into models of paper strength, since the force distribution will depend in a non-linear manner on the number of contacts for an individual fibre and their placement. These simulations do not take into account any bond breakage, as the sample is stretched. Simulations with bond breakage are more sensitive (22) to the configuration of the crossing fibres. Therefore it is important to perform sufficient simulations to obtain representative results. For further simulations presented in this paper, 30 simulations were performed and the results averaged.

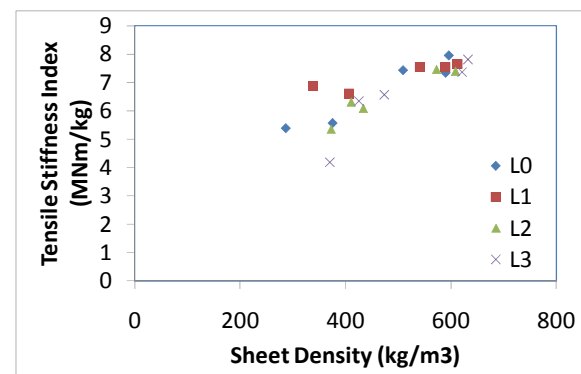


Figure 4 Tensile stiffness index versus density for samples L0-L3

Figure 4 shows the data of tensile stiffness index. The figure shows that firstly that tensile stiffness index increases with increasing sheet density, consistent with many sets of literature data. The figure also shows that fibre cutting has had a very small effect on the tensile stiffness, as had previously been found in the literature (11). The data is somewhat scattered and so difficult to make a precise estimate. For the purposes of the work here, the reduction in tensile stiffness from sample L0 to L2 is estimated to be 5% at constant sheet density. It is important to make the comparison at constant sheet density as if the fibre cross-sectional dimensions are constant then sheet density will be proportional to the level of bonding in the sheet. This set of data is important as it helps select the stress transfer coefficient,  $\beta$ .

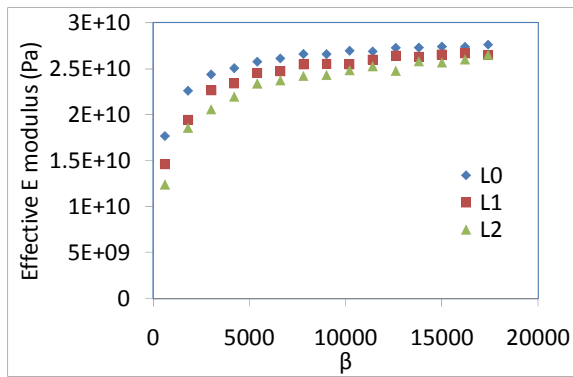


Figure 5 Effective elastic modulus versus  $\beta$  for L0-L2 at the same pressing level

Figure 5 shows the calculated effective elastic modulus. This was calculated from the average of 30 simulations by dividing the average stress in each fibre by the network strain applied. As mentioned previously the assumed elastic modulus of the fibre was 30 GPa. If the network strain was transferred through the end of the fibres and the transfer was perfectly efficient then the effective elastic modulus would match the fibre elastic modulus. The effective elastic modulus is always lower than the fibre elastic modulus as stress transfer is imperfect. It takes some distance from the end of the fibre before the strain in the fibre begins to approach the network strain. This figure shows that as  $\beta$  is reduced, then the effective elastic modulus in the fibre and thus the elastic modulus of the paper sample will also be reduced. The data also shows that the effect of fibre length becomes more important as the value of  $\beta$  is reduced. Whereas for  $\beta=17,000$ , the data for L0, L1 and L2 are almost coincident, it can be seen that for  $\beta=600$ , L2 is around 30% lower than L0.

The data here is an important, because by comparing with the tensile stiffness index data shown in Figure 4 we can estimate the value of  $\beta$ . The data in Figure 4 show that the tensile stiffness index of L0 is only around 5% higher than that of L2, at the same sheet apparent density. From this it can be concluded that quite a high stress transfer coefficient of 15,000 is required to produce the observed small difference in tensile stiffness index between sheets made from the different length fibres. This stress-transfer coefficient was used for all the simulations presented in this paper.

In order to simulate the fracture of paper, it is also necessary to know the fibre-fibre shear bond strength. As mentioned in the literature review, experimental values ranging over an order of magnitude have previously been obtained. The simulation technique described here was to investigate the effect of bond strength on the peak load in the fibre and compare it to the maximum

breaking load in the fibre estimated from the zero-span tensile strength. The value of  $\beta=15,000$  estimated from the elastic modulus data was used for the simulations. For the simulations, contacting fibres were generated according to the Weibull distribution for distance between contacts for the sample. The measurements also included the fraction of contacting fibres that were full contacts. Each contact was randomly selected to be a full or partial contact according to the measured data. The load distribution in the fibre was then calculated with a matrix strain of 0.002-0.005, depending on the bond strength chosen. Following this the load at each contact was then compared to the breaking load of a contact,  $F_b$ , which is given by

$$F_b = f \sigma_b D_w^2 / \sin \theta_{av} \quad (8)$$

where  $\sigma_b$  is the fibre-fibre shear bond strength,  $D_w$  is the fibre width,  $\sin \theta_{av}$  is the average crossing angle for two fibres and  $f$  is a fraction that was randomly generated between 0 and 1, if a contact was a partial contact, and was set to 1, if the contact was a full contact. If the breaking load of any contact was exceeded then it was removed from the calculation and the load distribution in the fibre recalculated. This process was repeated until the load at each contact was less than the breaking load of the bond. The external matrix strain was then incremented by the value of the initial matrix strain and the procedure repeated. The calculated data are presented as the peak load at the middle of the fibre versus the network strain. Each data point was the average of 30 simulations. Simulations were conducted with shear bond strengths ranging from 5 to 30 MPa, in steps of 5 MPa. Fibre fracture was not included.

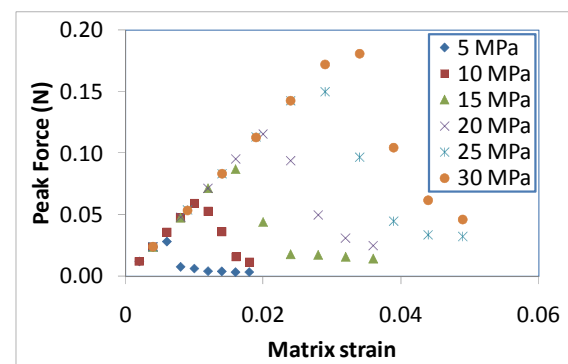


Figure 6 Peak load in the middle of the sample as a function of network strain for sample L0

Figure 6 shows the results of the simulations. The initial slope of the curve is the same for all simulations, as the initial slope depends solely on fibre elastic modulus,  $\beta$ , and the density of fibre-fibre contacts. The simulations are of interest, because they can be used to make some inferences about the fibre-fibre bond strength. Recall from

Table 2 that the estimated fibre breaking load calculated from the zero-span strength is 0.129N, it can be seen that a minimum bond strength of 25 MPa is required in order to achieve maximum loads in the middle of the sample sufficient to break the fibre, which observations of the fracture line show is occurring. This suggests that most literature values are far too low and have probably been influenced more by shear and rotation in the joint rather than providing a true value of the shear-bond strength. It is interesting that the highest estimates of bond strength from the literature were done by acid exposure measurements on sheets of paper and testing the sheets to infer a bond strength value of 29 MPa (27), based on weakening the sheet to the point where the strength of a fibre is equal or less than the strength of a single fibre-fibre bond. Based on the data in Figure 6, a bond strength of 25 MPa was then selected to calculate the average force along the fibre as a function of network strain

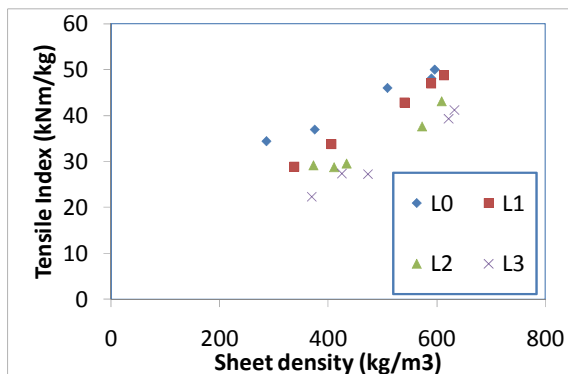


Figure 7 Tensile index versus sheet density for samples L0-L3

Figure 7 shows a graph of strength versus density for L0-L3. The data confirms previously measured trends in the literature that both fibre length and sheet density have an important effect on sheet strength. The effect of cutting the fibre to reduce the length weighted fibre length to 1.79 mm for L3 has been to reduce the sheet strength by around 50%. This shows quite a different trend to the elastic modulus data, which was almost independent of fibre length. The question is then can we explain the differences in trend with fibre length for elastic modulus and strength from the simulations?

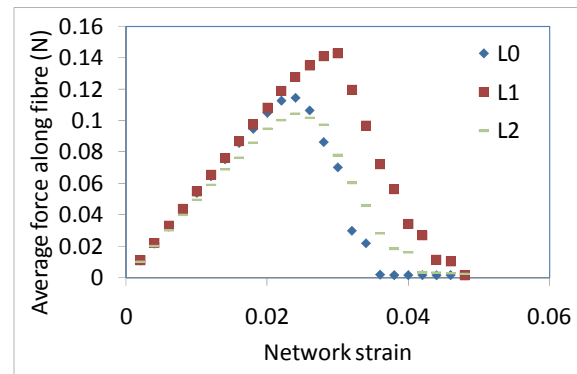


Figure 8. Average force along a fibre as a function of network strain for LO-L2

Figure 8 shows the average force as a function of network strain using a bond strength of 25 MPa. The simulations used the same methodology as was used for Figure 6, but calculating the average load along the whole fibre length, rather than the peak load in the middle of the fibre. The results are shown in Figure 8 for L0-L2. It can be seen that currently the differences between elastic modulus and strength cannot be explained through the simulations. There are only relatively small differences between the curves for each of the fibre length. The reason seems to be that with the high stress transfer coefficient, the maximum load is determined by the strength and concentration of the contact points at the end of the fibre. These are very similar for L0-L2 as the sheet density and contact statistics given in Table 1 and 2 are similar. The result was surprising but was confirmed by artificially reducing the number of contacts by increasing the Weibull parameter,  $b$ , by 50% and 100%, to decrease on average the number of contacts by 33 and 50%, respectively, while keeping all other factors constant and then repeating the simulations. The results are shown in Figure 9 and clearly demonstrate the effect of reducing the density of the network, which is as expected and confirmed by the data in Figure 7. The reasons for the discrepancy between the theoretical and experimental effect of fibre length, probably lie in the assumption that when the force at a bond exceeds the breaking load, the bond will then completely fail. At a minimum, this assumption will ignore frictional effects from the dry bonds in contact with each other.

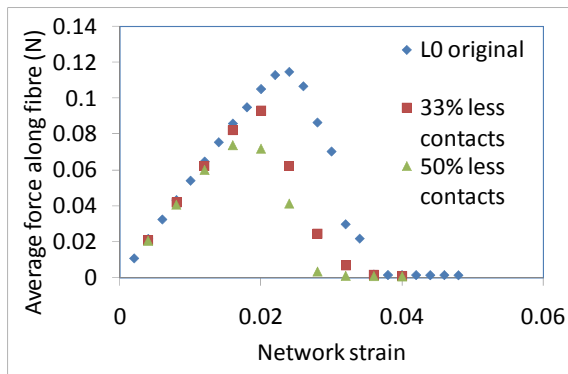


Figure 9 Effect of removing 33% and 50% of the contacts of the L0 sample on the average force as a function of network strain.

## CONCLUSION

A new method to calculate the force distribution in a loaded fibre network has been described. Measured force distributions were compared against experimental data obtained by wet fibre cutting to reduce the fibre length. The comparison of simulation and experimental data suggests that most literature values for fibre-fibre shear bond strength are too low.

## REFERENCES

- (1) Dent, R.W. - *J. Text. Inst.*, **92**(1):63 (2001)
- (2) He, J., Batchelor, W.J., and Johnston, R.E. - *Appita J.*, **57**(4):292 (2004)
- (3) Norman, R.J. - **Consolidation of the paper web transactions of the symposium held at cambridge, september 1965**, Bolam, F., Ed., 269: Technical Section of the British Paper and Board Makers' Association, London (1966)
- (4) Nordhagen, H., Eriksen, Ø., and Gregersen, Ø.W. - *Nordic Pulp Paper Res. J.*, **23**(2):189 (2008)
- (5) Gurnagul, N., Ju, S., and Page, D.H. - *J. Pulp Paper Sci.*, **27**(3):88 (2001)
- (6) Batchelor, W., Kibblewhite, R.P., and He, J. - *Appita J.*, **61**(4):302 (2008)
- (7) Joshi, K.V., - **A new method for shear bond strength measurement**, Masters Thesis: Chemical Engineering, Monash University (2007)
- (8) Batchelor, W.J., Westerlind, B.S., Hagglund, R., and Gradin, P. - *TAPPI J.*, **5**(10):3 (2006)
- (9) Hagglund, R., Gradin, P.A., and Tarakameh, D. - *Exp. Mech.*, **44**(4):365 (2004)
- (10) Van Den Akker, J.A., Lathrop, A.L., Voelker, M.H., and Dearth, L.R. - *Tappi*, **41**(8):416 (1958)
- (11) Niskanen, K., - **Paper physics**: Fapet Oy, Helsinki (1998)
- (12) Cox, H.L. - *British Journal of Applied Physics*, **3**(3):72 (1952)
- (13) Page, D.H. and Seth, R.S. - *Tappi*, **63**(6):113 (1980)
- (14) Page, D.H. and Seth, R.S. - *Tappi*, **63**(10):99 (1980)
- (15) Åström, J., Saarinen, S., Niskanen, K., and Kurkijärvi, J. - *Journal of Applied Physics*, **75**(5):2383 (1994)
- (16) Räisänen, V.I., Alava, M.J., Niskanen, K.J., and Nieminen, R.M. - *Journal of Materials Research*, **12**(10):2725 (1997)
- (17) Page, D.H. - *Tappi*, **52**(4):674 (1969)
- (18) Shallhorn, P. and Karnis, A. - *Transactions of the Technical Section (CPPA)*, **5**(4):TR92 (1979)
- (19) Carlsson, L.A. and Lindstrom, T. - *Composites Science and Technology*, **65**(2):183 (2005)
- (20) Kelly, A. and Tyson, W.R. - *Journal of the Mechanics and Physics of Solids*, **13**(6):329 (1965)
- (21) Kettunen, H. and Niskanen, K. - *J. Pulp Paper Sci.*, **26**(1):35 (2000)
- (22) Batchelor, W.J. - *Mechanics of Materials*, **40**(12):975 (2008)
- (23) He, J., Batchelor, W.J., and Johnston, R. - *TAPPI J.*, **2**(12):27 (2003)
- (24) He, J., - **Quantitative study of paper structure at the fibre level for the development of a model for the tensile strength of paper**, PhD Thesis: Dept. of Chemical Engineering, Monash University (2005)
- (25) He, J., Batchelor, W.J., Markowski, R., and Johnston, R.E. - *Appita J.*, **56**(5):366 (2003)
- (26) Page, D.H., El-Hosseiny, F., Winkler, K., and Bain, R. - *Pulp Paper Mag. Can.*, **73**(8):72 (1972)
- (27) Joshi, K.V., Batchelor, W.J., Parker, I.H., and Nguyen, K.L. - **International Paper Physics conference**, Batchelor, W.J., Ed., 7: Appita, Gold Coast (2007)